Evolution of Precipitates during Age-hardening of AW 6016 Alloy

R. Schiffmann, J. Haug, J. Banhart

Hahn-Meitner Institute, SF3,Glienicker Straße 100
D-14109 Berlin-Wannsee, Germany

Abstract

Specimens of a sheet of the commercial age-hardening aluminium alloy 6016 were heat-treated in order to produce different hardening stages. By neutron small angle scattering (SANS) the precipitation sequence and its development in the nanometer range can be monitored. Transmission electron microscopy (TEM) serves as an additional tool. Variations in the precipitation sequence are observed at different age-hardening temperatures. Mechanical properties such as hardness and strength are modified due to the nanostructural precipitation process.

1. Introduction

In view of their use as sheet material for car body applications growing effort is put on investigating aluminium 6xxx alloys. Their bake-hardening capabilities have been known for quite some time [1]. Although reproducible results for hardness and strength increase can be achieved still some controversy persists on the micro- and nanostructural processes producing this effect [2]. Better understanding of these processes will certainly be helpful in further alloy development and application.

The precipitation sequence occurring in solution-treated and quenched material during age-hardening is reported to be: clusters → GP-zones → β"- and β'-phases, and finally the stable Mg_2Si-phase β. Even absence of some of the different steps of the precipitation sequence is reported at low age-hardening temperatures [3]. The nature of these clusters depends on the alloy composition and the Si- or Mg-excess. The limit between 'clusters' and spherically shaped G.P.I-zones is taken to be the size at which visibility in the TEM is reached [4]. Cluster formation starts in the first moments of age-hardening, after which the formation of non-spherical G.P.II zones and rod-shaped β'-precipitates in <100> direction follows. It can be assumed that the rods evolve from clusters. They usually grow faster in thickness than in longitudinal direction [5]. Precipitate formation and transformation processes terminate with the stable, platelet-shaped Mg_2Si-phase β, see e. g. [6].

In this study the detection of early-stage precipitation is primarily attempted by means of small angle neutron scattering (SANS). Additional investigations such as transmission electron microscopy (TEM) help to confirm the findings. Micro-hardness measurements (HV) yield the macroscopic mechanical properties to be correlated to microscopically observed phases. SANS investigations of age-hardening in aluminium 6082 alloys have been carried out previously [7], but as the work is only concerned with modifications in neutron scattering behaviour caused by different heat treatments without including metallurgical and microstructural details the results are too inconclusive for our purposes.

Donnadieu and co-authors [8] monitored precipitate formation by SANS and TEM investigations in a very thorough study. As only one age-hardening state is treated and compared to a reference state nothing is said about the evolution of the precipitates in time.

2. Experimental Procedures

The investigated material was an EN-AW6016 sheet of 1.2 mm thickness supplied by Hydro Aluminium. The chemical composition is given in Table 1. This alloy contains 0.63 % Mg_2Si and a Si-excess of 1.21 %. This is calculated according to the formula in [9] taking into regard Fe content which leads to FeSi precipitates.

Table 1: Chemical composition of the EN-AW6016 sheet material (determined by neutron activation analysis and elastic recoil detection analysis).

element	Al	Mg	Si	Fe	Mn	Zn	Cr
mass-%	98.4	0.41	1.5	0.23	0.069	0.013	0.0073

The age-hardening times and temperatures after solutionizing and quenching applied for preparing specimens for SANS and TEM are given in Table 2.

Table 2: Age-hardening cycles of the alloy 6016 (after solutionizing for 1 h at 540°C and quenching in water at 20°C)

Temperature	185°C	235°C
Times	5 min	5 min
	25 min	10 min
	90 min	28 min
	5 h	60 min
	27 h	120 min

The specimen dimensions were 15x15 mm^2 for both hardness and SANS measurements. TEM specimens were ground and polished by HNO_3-CH_3OH electrolyte to 3 mm discs of about 100 µm thickness. In addition to these samples, specimens were prepared for simple hardness measurements by age-hardening at 120°C, 140°C, 165°C, 185°C, 205°C, 225°C and 245°C for a variety of times.

3. Experimental Results

3.1 Hardness

A micro-hardness tester was used to determine the hardness for each ageing stage. Applying a simple parabolic fit function to the time-hardness-curves at each temperature level it can be found that the maximum hardness at the lower temperature is achieved after about 3 to 4 h, at the higher temperature after about 10 to 20 min. Therefore the investigated heat treatment cycles include the complete range from under-aged to over-aged conditions. The maximum hardness values of this material are shown as a time-temperature-diagram in Figure 1. Maximum hardness is assumed around ~180°C and 2 to 3 hours.
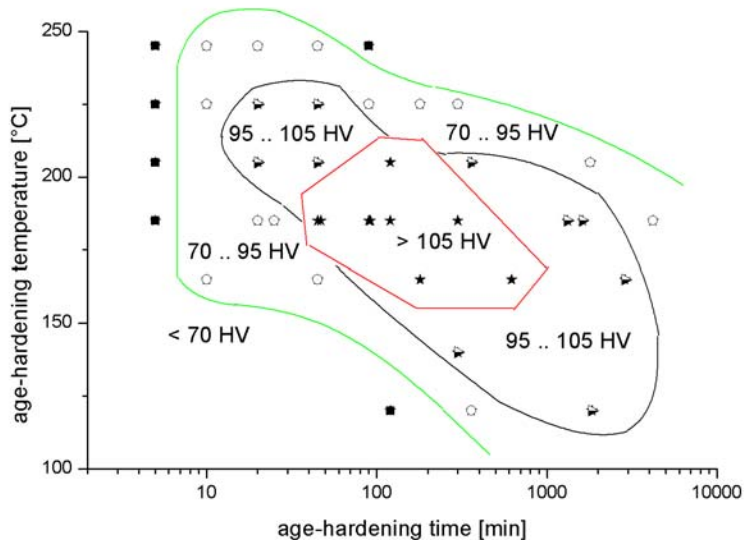
Figure 1: Time-temperature-hardness diagram of 6016 alloy.

3.2 Small angle neutron scattering (SANS)

If a sample is heterogeneous with fluctuations of the composition and/or density occurring in a microscopic size scale, i. e. 0.5-400 nm, a small angle scattering effect can be observed [10]. SANS was carried out at the BER II reactor of the Hahn-Meitner-Institute Berlin using instrument V4. The experiments were performed over three sample-detector distances using a neutron wavelength of λ=0.605 nm to cover a Q-range from 0.02 to 3.8 nm^{-1}. The measured data were corrected and normalized to absolute units by using water as calibration standard [11]. In order to achieve sufficient neutron scattering four sheets of 15x15x1.2 mm of the same heat treatment were stacked on top of each other.

The neutron scattering cross sections for the two temperature series 185°C and 235°C applying different age-hardening times are given in Figure 2. At larger Q-values around Q=1.1 nm^{-1} small angle scattering from precipitates with a size of about 2 nm occurs. For the 185°C series these precipitates grow with time (the maximum is shifted to smaller Q-values). The 235°C series shows scattering functions in this Q-range similar to that of 185°C/5h specimen. A spherical shape for these small precipitates was assumed and the experimental data were fitted with a log-normal distribution function of the radius. As an example, Figure 3 gives the log-normal distribution corresponding to an age hardening temperature of 185°C. The mean radius R is increasing with hardening time and the distributions get wider. Figure 4 shows the development of the growing precipitates, (a) for the lower and (b) for the higher age-hardening temperature. The maximum of the radius distributions and the volume fraction are plotted over age-hardening time. The size and volume fraction of the precipitates grow with increasing age-hardening time and the values are higher for age-hardening at 235°C.
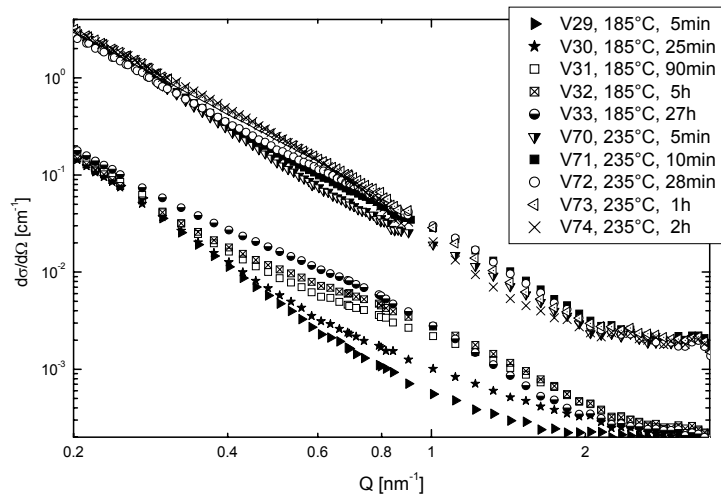
Figure 2: SANS function of specimens age-hardened at 185°C and 235°C (plots for 235°C are shifted up by one order of magnitude).
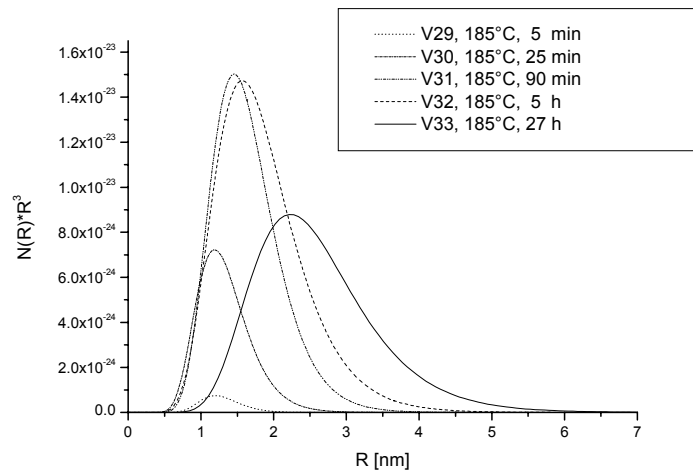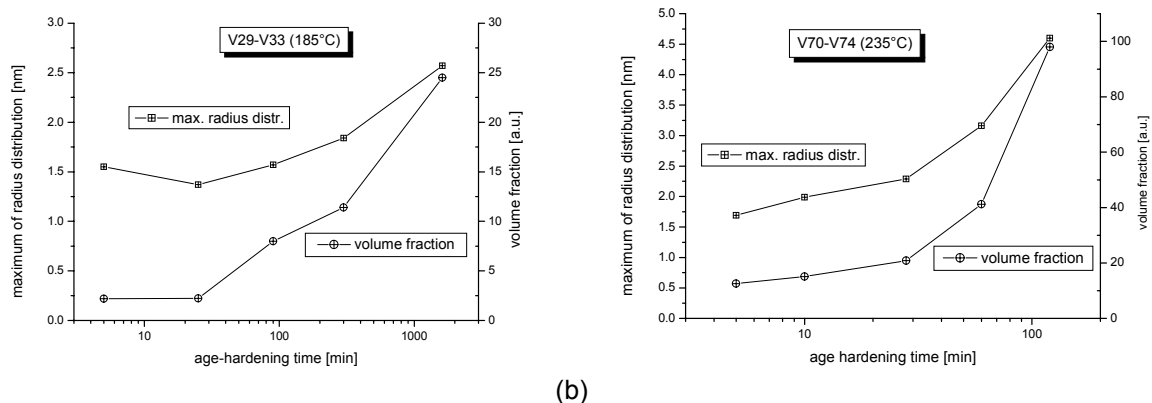

Figure 3: Log-normal distributions of spherical scatterers in 6016 alloy hardened at 185°C.

(a)   (b)

Figure 4: Growth in size (maximum of the radius distribution) and volume fraction of precipitates in samples age-hardened at (a) 185°C and (b) 235°C.

3.3 Transmission electron microscope imaging (TEM)

An example of typical needle-shape precipitates in a sample at maximum hardness is shown in Figure 5. The precipitates are about 20 to 50 nm long and a few nm thick. At age-hardening temperatures above 200°C streaks typical for rods or needle-shaped

objects were observed in the electron scattering images (SAED). In this case they are produced by objects parallel to the <100> directions. At lower ageing temperature (e. g. 185°C) needle-shaped precipitates are rarely observed in TEM and no streaks appear in the SAED-image.

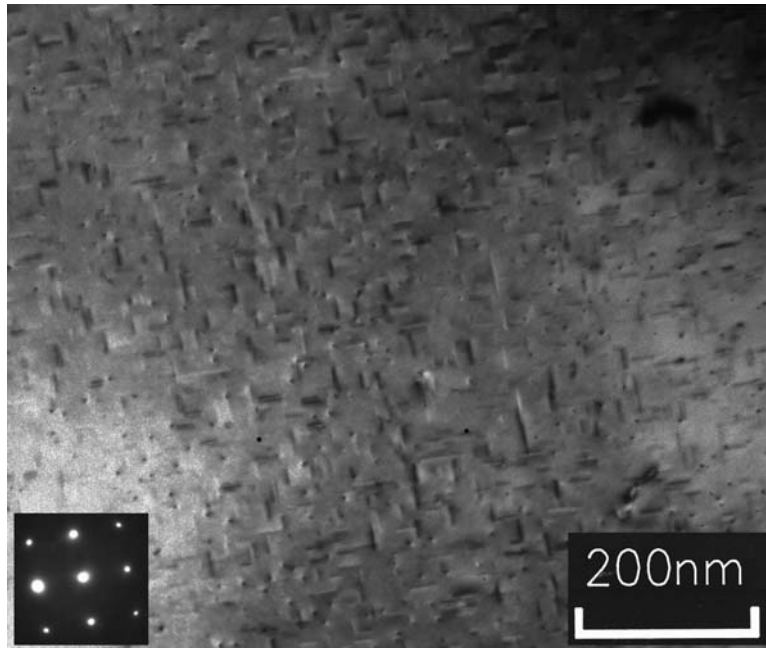Figure 5: Bright field image of typical needle-shaped precipitates (aged at 225°C for 10 min).

4. Discussion

Early stage precipitates in Al-Mg-Si alloy can be detected by small angle neutron scattering (SANS). They grow with age-hardening time. Comparing these SANS results with hardness measurements and knowing that rods are partly responsible for hardening it is clear that the small precipitates will represent the β''-phase. The highest hardness for 185°C (age-hardening time 90 min and 5 h) corresponds to particles with about 4 nm diameter in SANS, the highest hardness for 235°C (measured after 10 min and 28 min age-hardening) yield the same particle size in SANS measurements. For longer aging times the size of the precipitates grows and the hardness decreases. For shorter times the volume fraction of the precipitates is too low to produce higher hardness values. To calculate the radius and length of these rods the SANS data should be fitted with a log-normal distribution function for cylinders. For the samples age-hardened at 235°C hardness decreases in the over-aged state because the volume fraction of the small precipitates decreases. In general a marked influence of the temperature on the precipitation sequence is found. Remarkably, the achieved hardness is higher at the lower age-hardening temperature although the traditional precipitation sequence as reported in the literature is not obeyed so well. Moons et al. [3] explain this effect by the high Si-excess of the investigated 6016 alloy and call it 'cluster strengthening'. Furthermore, a quite short age-hardening time (3 to 4 h) to achieve a relatively high strength (110 HV corresponding to $R_m \approx 290$ MPa) is found compared to other series 6xxx alloys.

5. Conclusions

A refined analysis of the presented SANS data based on cylindrical instead of spherical particles will be applied. In order to further clarify the structures, shapes and compositions

of the precipitates atom probe investigations (APFIM) of the age-hardened specimens are in preparation. Especially early-stage clusters and needles should be detectable by this method. The Si-excess will be varied to assess its influence on the precipitation sequence and rate. An EN-AW6060 alloy having half the Si-content of the material in this study is already being investigated.

Acknowledgements

References

[1]   P. Brenner and H. Kostron, Z.Metallkde. Bd.31(1939), S.89/97, Über die Vergütung der Aluminium-Magnesium-Silizium-Legierungen (Pantal).
[2]   G.A. Edwards, K. Stiller, G.L. Dunlop and M.J. Couper, Acta mater. Vol.46(1998), No.11, pp.3893-3904, The precipitation sequence in Al-Mg-Si alloys.
[3]   T. Moons, P. Ratchev, P. De Smet, B. Verlinden and P. Van Houtte, Scripta Materialia, Vol.35(1996), No.8, pp.939-945, A comparative study of two Al-Mg-Si alloys for automotive applications.
[4]   M. Murayama and K. Hono, Acta Mater. Vol.47 (1999) pp. 1537-1548, Pre-precipitate clusters and precipitation processes in Al-Mg-Si alloys.
[5]   A.K. Gupta, D.J. Lloyd and S.A. Court, Materials Science and Engineering A301(2001), pp.140-146,Precipitation hardening processes in an Al-0.4%Mg-1.3%Si-0.25Fe aluminium alloy.
[6]   M.H. Jacobs, The Philosophical Magazine - a journal of theoretical, experimental and applied physics, eight series-Vol.26(1972), p.1-13, The Structure of the Metastable Precipitates Formed During Ageing of an Al-Mg-Si Alloy.
[7]   G. Albertini, G. Gagliotti, F. Fiori and R. Pastorelli, Physica B 276-278(2000), pp. 921-922, SANS investigation of precipitation in heat-treated AA6082 alloy.
[8]   P. Donnadieu, F. Carsughi, A. Redjaima, C. Diot and G. Lapasset, J. Appl. Cryst. (1998). 31, 212-222, Nanoscale Hardening Precipitation in AlMgSi Alloys: a Transmission Electron Microscopy and Small-Angle Neutron Scattering Study.
[9]   A.K. Gupta, D.J. Lloyd and S.A. Court, Materials Science and Engineering A316(2001), pp. 11-17,Precipitation hardening in Al-Mg-Si alloys with and without excess Si.
[10] A. Guinier and G. Fournet, John Wiley & Sons, New York, 1955, Small-Angle Scattering of X-rays.
[11] U. Keiderling, Appl. Phys. A 74 [Suppl.] (2002) S1455-1457, The new "BerSANS-PC" Software for Reduction and Treatment of Small Angle Neutron Scattering Data.